

HIGH HEAT FLUX SENSORS CALIBRATION IN A COOLED ENCLOSURE

by

Annageri V. Murthy

Aero-Tech, Inc.

53 Sanlun Lakes Drive

Hampton, VA 23666, USA

and

Benjamin K. Tsai and Robert D. Saunders

National Institute of Standards and Technology

Gaithersburg, MD 20899, USA

**Rerinted from the Instrumentation Symposium, 45th International.
Proceedings. Sponsored by Aerospace Industries Division and Test Measurement
division of ISA. May 2-6, 1999, Albuquerque, NM, 91-100 pp, 1999.**

**NOTE: This paper is a contribution of the National Institute of Standards and
Technology and is not subject to copyright.**

NIST

National Institute of Standards and Technology
Technology Administration, U.S. Department of Commerce

High Heat Flux Sensors Calibration in a Cooled Enclosure

A. V. Murthy
Aero-Tech, Inc.,
Hampton, VA 23666

B. K. Tsai
Nat'l Inst of Stds and Tech
Gaithersburg, MD 20899

R. D. Saunders
Nat'l Inst of Stds and Tech
Gaithersburg, MD 20899

KEYWORDS

Absolute technique, Calibration, Heat flux, Radiation, Sensor, Transfer technique

ABSTRACT

This paper reports results of an experimental study of calibrating heat flux sensors using a spherical blackbody and mounting the sensor inside a cooled outer sleeve protruding from the radiating aperture. Measurements with a Gardon-type heat flux sensor show that this arrangement may not necessarily lead to improved absolute calibrations at all locations inside the cooled sleeve. Large variations in measured responsivities were observed depending on the distance of the gage from the radiating aperture of the blackbody. These variations are suspected to be due to the induced circulation effect of the furnace hot gas extending up to the gage location. It is demonstrated that the variations can be reduced by providing suitable venting around the gage holder instead of testing in a fully closed mode. However, transfer calibration of the same Gardon gage with a reference standard Schmidt-Boelter gage gave good agreement for gage locations ranging from inside the furnace to well within the cooled enclosure. Limitations of the testing in the cooled enclosure and possibilities for further improvement are discussed.

INTRODUCTION

Development of radiative calibration facilities using blackbodies to provide traceable calibration of heat flux sensors is in progress at the National Institute of Standards and Technology (NIST). Reference 1 gives an overview of the various methods in use and under development. The method currently in use for calibrating sensors up to about 50 kW/m^2 uses a transfer standard electrical substitution radiometer (ESR) and a blackbody radiant source. This method, generally referred to as the 'transfer calibration,' involves several successive stages [2] of calibration with traceability to a cryogenic radiometer [3] - the primary standard for optical radiation in the U.S. When sensors are calibrated in vacuum, the net heat flux at the sensor surface is determined by the balance of the radiant heat flux absorbed at the surface and the re-radiation of energy from the sensor surface. Generally, re-radiation effects are small when the temperature of the radiant source is much higher than the sensor surface temperature. Further, the re-radiation effects can be calculated, if necessary, to determine the net heat flux at the sensor surface.

Sensor calibration under conditions other than vacuum can introduce additional modes of heat transfer at the sensor surface depending on the temperature difference between the sensor surface and the surrounding environment. The situation with the sensor being calibrated in an open mode in ambient air

represents a classical example of heat loss due to free convection from a heated surface. However, when the sensor is close to the furnace or exposed to hot gases exiting from a high temperature blackbody, the determination of net heat loss or gain from the sensor surface to the surroundings can be difficult. In the transfer calibration technique, as long as the convective effects are similar for both the transfer standard and the sensor to be calibrated, the calibration is not likely to be significantly affected. However, if the calibration of the sensor is to be determined absolutely from blackbody radiation calculations, it is necessary to quantify the contribution of other modes of heat transfer.

Convection effects tend to increase when the sensors are located close to the radiating aperture because of exposure to hot gases from the furnace. This situation occurs when calibrating sensors in the heat flux range of 100 kW/m^2 and at source temperatures of approximately 1200 K. Calibration of sensors in this range of heat flux is of interest in fire research and testing. A method to minimize the convection effects under these calibration conditions was proposed by Olsson [4,5]. The method, referred to as 'cooled-enclosure,' is comprised of a water-cooled outer sleeve enclosing the radiating aperture and the sensor to be calibrated. The method used a spherical blackbody with a water cooled-aperture as the radiant heat flux source. Since the sensor was housed inside the cooled surrounding, the convection effects were assumed to be small. The heat flux at the sensor surface was calculated by radiation balance within the enclosure. The method is simple and eliminates error propagation present at various stages in the transfer calibration technique.

An experimental study was initiated at NIST recently to evaluate the feasibility of using the cooled enclosure technique to calibrate high heat flux sensors. The study was motivated because of the need to calibrate sensors at source temperatures used in fire research and test methods. In addition, the cooled enclosure was expected to provide a more favorable test environment for transfer calibrations by reducing stray radiation effects from the aperture surroundings. A prototype facility using a spherical blackbody with a cooled aperture has been built. This facility is now in operation and preliminary measurements have been made using a cooled Gardon sensor and an uncooled Schmidt-Boelter type sensor. This paper describes the facility and presents preliminary findings on the use of the cooled-enclosure technique for both a transfer standard source and an absolute calibrator. Limitations of the method and possibilities for further improvement are discussed.

FACILITY DESCRIPTION

Figure 1 shows a schematic layout of the spherical blackbody facility and the associated cooled enclosure housing the sensor to be calibrated. The blackbody cavity is a spherical furnace, 0.23 m diameter, and is fitted with a 50.8 mm diameter radiating aperture. The furnace walls are made of clay and are electrically heated. The furnace inner surface is coated with a high temperature black paint. The furnace can be operated continuously up to a maximum temperature of 1373 K. Operation at higher temperatures up to 1446 K is possible for shorter duration. The cavity temperature is measured by a precision type S thermocouple. A PID controller maintains the cavity temperature at a set value within 1 K. Provision for computer control of the temperature is available through a serial RS-232 interface. The exterior of the furnace is air cooled and the maximum power requirement is 1.5 kW. With the present design, the facility is operated in an upright position with the radiating aperture in the vertical plane.

The cooled enclosure is comprised of a single-piece water-cooled extension tube with a precision aperture at one end fitted to the radiating cavity of the spherical furnace. The other end serves as an opening for inserting the sensor housing assembly. The inside of the tube is coated with a high temperature black paint with an emissivity of about 0.93 to 0.94. The cooled extension tube minimizes effects of reflected radiation from the inner surface of the tube on to the sensor surface. A stop ring on the inner surface at a distance of 12 mm from the aperture end helps to precisely locate the sensor assembly inside the tube. Four type K thermocouples are located 90° apart on the inner surface of the tube, midway between the aperture and the stop ring. The spherical blackbody furnace and the extension tube forming the cooled enclosure were fabricated by Mikron Instrument Company.¹

The radiating aperture and the extension tube are water-cooled continuously by a recirculating chiller. The chiller consists of an air-cooled refrigeration system, a closed water reservoir, a recirculating pump and temperature controller. The recirculating pump is of positive displacement type and the flow rate is 14 L/m at about 1.4 bar pressure. The cooling water temperature range is from +5 °C to +30 °C. During tests, the controller is set to maintain cooling water temperature at 25 °C to avoid condensation.

Figure 2 shows the gage housing assembly consisting of an outer sleeve and a positioning sleeve. The outer sleeve slides up to an aperture stop on the cooled extension tube assembly of the furnace. The gage to be calibrated is mounted at one end of a positioning sleeve. The gage can be located at different distances from the aperture by using spacer rings. The positioning sleeve slides inside the outer sleeve and the complete assembly fits into the cooled extension tube from the furnace forming a closed cooled enclosure for the gage to be calibrated.

The outer sleeve is slotted to prevent fouling with the surface-mounted thermocouple lead wires. Figure 2 shows a typical assembly with a 25-mm diameter Gardon gage located at a distance of 12.5 mm from the radiating aperture. Other types of gages, up to a maximum diameter of 25 mm, can be mounted to the positioning sleeve using suitable adapters. By using different size spacer rings, the gage can be located at known distances from the radiating aperture. With the present design and location of the sensor, it is expected that heat flux sensors can be calibrated up to 100 kW/m², at a maximum source temperature of approximately 1373 K.

APERTURE EMISSIVITY

The theoretical total emissivity ϵ_o of an aperture in a cavity can be calculated using Gouffe's method [6]. The general expression for the emissivity is given by the equation,

$$\epsilon_o = \epsilon (1 + k) / [\epsilon (1 - A_1/A_S) + (A_1/A_S)] \quad (1)$$

where $k = (1 - \epsilon) [(A_1/A_S) - (A_1/A_{S_o})]$
 $\epsilon =$ emissivity of materials forming the blackbody surface

¹ 16 Thornton Road, Oakland, NJ 07436. Certain commercial equipment, instruments, or materials are identified in this paper to foster understanding. Such identification does not imply recommendation or endorsement by the National Institute of Standards and Technology, nor does it imply that the materials or equipment are necessarily the best available for the purpose.

- $A_1 =$ area of the aperture
- $A_s =$ area of sphere inner surface
- $A_{so} =$ surface area of a sphere of same depth as the cylindrical cavity in the direction normal to the aperture

The value of constant k is nearly zero for most cavity shapes. For the present spherical blackbody, the cavity diameter is 23 cm, and the aperture diameter is 5.1 cm. For this geometry, assuming $k = 0$, the calculated values of the total emissivity (ϵ_o) are 0.9969, 0.9986 and 0.9994 for emissivity (ϵ) values of 0.8, 0.90 and 0.95, respectively. Even with a lower value of 0.8 for the emissivity of the blackbody cavity surface coating material, the calculated total emissivity ϵ_o is 0.997. However, it must be noted that the method does not take into account the localized effect of the cooled aperture or temperature variations on the sphere surface. The uncertainties involved due to the cooling effect are difficult to estimate, and are not considered in the analysis.

ENCLOSURE RADIATION MODEL

The heat flux at the sensor surface is calculated considering the radiation balance in the enclosure bounded by the radiating aperture, the cooled extension tube, and the sensor to be calibrated. Figure 3 shows the schematic layout of the enclosure showing the gage location with respect to the radiating aperture. The enclosure model consists of five radiating surfaces designated 1 to 5 in Fig. 3. Designation 1 and 5 refer to the radiating aperture and the sensor surface, respectively. Designation 4 refers to the annular disc area between the gage and cooler section. The cooler section is considered to be comprised of two parts, designated by 2 and 3, for computational purposes. The enclosure model represents closely the experimental conditions since there are no view-limiting apertures on the sensor or an inner cooler surrounding the gage body. The equation for the net radiation in the enclosure is given by [5,7],

$$(q_i/\epsilon_i) - \sum_{k=1,5} [(1 - \epsilon_k)/\epsilon_k] F_{ik} q_k = \sum_{k=1,5} \sigma F_{ik} (T_i^4 - T_k^4) \quad (2)$$

where q is the net radiation per unit area leaving the surface, F_{ik} configuration factor representing fraction of radiant energy incident on surface k from surface i , ϵ surface emissivity, T surface temperature and σ the Stefan-Boltzmann constant. The subscripts i, k refer to surfaces forming the enclosure.

Figure 3 shows a typical location of the gage from the radiating aperture. In the position closest to the aperture, the sensor is located in the plane of the aperture stop. In the second position, the sensor can be placed 1.64 cm farther away from the aperture. With suitable spacers, the gage can be located at other positions, if necessary. Table I gives the relevant dimensions for the enclosure geometry for the gage locations used in the present experiments.

The temperatures of surfaces 1 to 5 are assumed to be known and are either measured or calculated. The emissivity of the aperture is given by equation (1). The emissivities of other surfaces, which are obtained from the characteristics of the paint, usually vary from 0.7 to 0.9. The configuration factors F_{ik} between various surfaces are calculated from the geometry of the enclosure. The set of equations

defined by equation (2) for $i = 1$ to 5 are solved to determine the unknown heat flux for each surface i . For a specified furnace temperature and the corresponding cooler section temperatures, the heat flux value at the sensor to be calibrated is given by q_5 .

Table I. Enclosure geometry and surface areas.

Surface		Gage position (L_2+L_3)								
		I (1.27 cm)			II (2.91 cm)			III (4.70 cm)		
Name	i or k	D cm	L cm	Area cm^2	D cm	L cm	Area cm^2	D cm	L cm	Area cm^2
Aperture	1	5.08		20.3	5.08		20.3	5.08		20.3
Cooler - Sec. 1	2	5.24	0.63	10.4	2.62	1.27	20.9	5.24	1.27	20.9
Cooler - Sec. 2	3	5.24	0.63	10.4	2.62	1.64	27.0	5.24	3.43	56.4
Gage housing	4	5.24		21.6	2.62		21.6	2.62		21.6
Gage surface	5	0.50		0.20	0.25		0.20	0.25		0.20

A Visual Basic™ program was developed to solve the net radiation balance equation (2) to determine the heat flux at the sensor surface. The data corresponding to test conditions of reference 5 was used to check the calculation method. The method followed is similar to that described in reference 5. However, in the present setup, there are no view-limiting apertures. Hence, the reflection terms from the cooler to the sensor are retained in the calculation.

RADIANT HEAT FLUX CALCULATIONS

The temperature on the cooler surface was measured at four circumferential locations 90° apart at a distance of 0.64 cm from the aperture. An empirical fit for the average of the four measurements was used in the radiation balance computations. Figure 4 shows the measured variation in the cooler temperature (T_c), with increasing furnace temperature, with the cooling water temperature (T_w) maintained at 25°C . It is assumed that the temperature distribution along the cooler length is uniform. This assumption will likely result in a slightly higher value of the heat flux calculated. Further improvements can be incorporated, if necessary, at a later date. However, the contribution of the cooler surface to the radiant heat flux at the gage is small, and the assumption of uniform temperature does not in any way affect the analysis of the present experimental results. Calculations were performed for three locations of the sensor in the cooled enclosure (Fig. 5). In the first position, the gage is in the plane of the aperture stop, 1.27 cm from the aperture. In the second and third positions, the gage is located further away at distances of 2.9 cm and 4.7 cm, respectively. Figure 6 shows the calculated heat flux level at the gage surface. High heat flux levels of up to about 150 kW/m^2 can be realized in the first location.

EXPERIMENTAL RESULTS

In the first series of experiments, a 25 mm diameter water-cooled Gardon gage without window was used. The output of the gage was recorded for approximately 60 s to 120 s after stabilization of the test

conditions following insertion of the gage assembly into the cooled enclosure. Figure 7 shows the output of the gage for three positions relative to the aperture (1.27 cm, 2.91 cm and 4.7 cm), against the calculated heat flux level for different furnace temperatures. The first observation from this data is that widely varying responsivities of the gage are found at different positions in the enclosure. The responsivity is about $0.084 \text{ mV}/(\text{kW}/\text{m}^2)$ in Position-I at distance of 1.27 cm from the aperture. The responsivity increases to about $0.097 \text{ mV}/(\text{kW}/\text{m}^2)$ and $0.129 \text{ mV}/(\text{kW}/\text{m}^2)$ when moved to Positions II and III, 2.91 and 4.70 cm from the aperture, respectively. This large increase in sensitivity by about 50 % cannot be attributed to either experimental uncertainties or errors, nor to approximations in the enclosure model. For a specified value of calculated radiant heat flux, the output of the gage is larger when moved away from the aperture to a cooler section of the enclosure. This means that the heat flux actually sensed by the gage is much higher than that predicted purely by radiation considerations.

The enclosure configuration can be considered as fully closed for purposes of radiation balance calculations. However, it is not completely sealed. The slots for taking thermocouple leads in the outer sleeve permit equalization of pressures when the gage assembly is inserted. Since the gage surface and the surroundings are at a much lower temperature than the furnace, it is likely that the hot gas from the furnace is creating a strong induced circulation within the enclosure. The flow due to induced circulation heats up the gage surface, resulting in increased heat flux. While the radiant heat flux at the gage surface is reduced as the gage is moved away from the aperture, the heat flux due to this induced flow effect does not reduce proportionately since the gage is in a closed enclosure. Also, when the gage is moved away from the aperture, to obtain the same level of radiant heat flux at the gage surface, the furnace has to be operated at a higher temperature. The operation at higher temperature leads to increased induced flow heat transfer relative to the radiant flux at the gage surface. The gage sensing surface temperature which depends on the type of sensor alters the heat transfer due to induced flow effects. When the difference between the gage surface temperature and the surrounding is small, the main contribution to the heat flux at the gage is the radiant mode. This situation is likely to prevail when the gage is located at or close to the aperture since the furnace is operated at a lower temperature to obtain the same level of radiant heat flux.

To examine whether the confined nature of the cooled enclosure was leading to the observed variations in the measured responsivities, the test was repeated with the outer sleeve removed. The relatively small opening around the gage holder with the removal of the outer sleeve does not affect radiant heat flux conditions at the gage surface. However, the opening provides for free flow of ambient air around the gage holder thus affecting the heat transfer due to induced flow effects:

The results of this test are shown in Fig. 8. Without the outer sleeve, the measured responsivities at the three locations are much closer compared to closed enclosure values with the outer sleeve mounted. In Position-I, 1.27 cm from the aperture, the responsivity without the outer sleeve is about $0.089 \text{ mV}/(\text{kW}/\text{m}^2)$, about 6 % higher than with outer sleeve. In Position-II, 2.91 cm from the aperture, the responsivity with and without the outer sleeve are almost the same at about $0.097 \text{ mV}/(\text{kW}/\text{m}^2)$. At the farther most Position-III, 4.7 cm from the aperture, the responsivity without the outer sleeve is about $0.106 \text{ mV}/(\text{kW}/\text{m}^2)$, about 20% lower than with the outer sleeve. While removing the outer sleeve does not eliminate the convection effects, it certainly is reducing the severity of the additional heat flux due to induced flow effects. This suggests that it will be interesting to test the gage with larger openings around the holder than in the present configuration. The larger opening will probably reduce induced

flow effects on heat flux at the sensor surface, leading to better agreement in measured responsivities at different gage distances from the aperture.

Figures 9a-c show a direct comparison of the effect of removing the outer sleeve on gage response for a fixed distance of the gage from the aperture location. The test results with and without the outer sleeve show that calibrating heat flux sensors in a fully closed cooled enclosure may introduce variations in the measured responsivity depending on the location of the gage inside the enclosure. When the gage was located in Position II, the measured responsivities with and without the outer sleeve agree closely. This observation suggests that it may be possible with more detailed investigation to identify the best location for the gage for use as an absolute calibrator.

The present results demonstrate that for the cooled enclosure technique to be used as an absolute calibrator, it is necessary that the convection effects are kept small. Tilting the test assembly so that the radiating aperture and the test sensor are in a horizontal plane will reduce convection effects to some extent. However, a complete understanding and quantification of the convection effects on the heat flux at the sensor surface is necessary for the absolute technique to be used successfully as a primary standard.

The cooled enclosure also provides a favorable environment for transfer calibration since the stray radiation from the aperture surroundings incident on the sensor is greatly reduced. Further, in transfer calibration, as mentioned in Section (2), the convection effects will have similar effects on both the reference standard and the test gage. Hence, a transfer calibration, discussed below, using a reference standard gage was carried out.

The reference gage was a Schmidt-Boelter sensor [8]. Over the past two years, this gage has been calibrated several times with respect to an electrical substitution radiometer and has shown repeatability of calibration within about 1.0 percent [9]. The heat flux measured by the Schmidt-Boelter sensor represents the total net flux at the sensor surface. The measurements were made in the completely enclosed mode with the outer sleeve at five locations. These locations include the three positions 1.27 cm, 2.91 cm and 4.7 cm from the aperture, discussed earlier. The other two locations were at the aperture plane (0.0 cm) and inside the furnace at a distance of 0.99 cm from the aperture. These locations cover extreme combinations of radiant and other modes of heat transfer at the gage surface.

Figure 10 shows the results of the transfer calibration. The measured responsivities at all five locations agreed within 2% of the mean value. The mean responsivity obtained from linear regression to the data in Fig. 10 is $0.095 \text{ mV}/(\text{kW}/\text{m}^2)$, with an estimated uncertainty ($k=2$) of about 3%. It must be noted that the five locations represent widely varying heat transfer - radiant and convective - conditions. Because of the different principles of operation, the response of the reference Schmidt-Boelter gage and the test Gardon gage to convection heat transfer are different. More detailed studies are planned to evaluate these effects. The responsivity of $0.097 \text{ mV}/(\text{kW}/\text{m}^2)$ obtained earlier by enclosure model calculations at Position-II (2.91 cm) differs by about 2 % from the mean responsivity from transfer calibration. The good agreement between the transfer calibration and the enclosure model data at Position-II suggests that the enclosure model technique might be improved by choosing an optimum location for the gage inside the enclosure. However, convection heat transfer in the enclosure, which determines the accuracy of absolute calibration, needs to be understood. Further, instead of a completely closed enclosure, a semi-

open mode using smaller size gage holders which provide adequate flow of ambient air around the enclosure may be preferable. With this arrangement, it may be possible to refine the absolute calibration technique.

CONCLUSIONS

A facility for calibrating high heat flux sensors in a cooled enclosure using a spherical blackbody has been developed. Measurements with a Gardon gage showed that when the enclosure is fully closed, the heat flux at the sensor location can be significantly affected by the furnace hot gas. Absolute calibration based purely on radiation balance within the enclosure can lead to variations in measured responsivity depending on the location of the sensor. It was demonstrated that these variations can be reduced by proper venting of the enclosure. Despite the varying level of other modes of heat transfer in addition to radiation in the enclosure, transfer calibration with reference to a previously calibrated Schmidt-Boelter sensor showed good agreement.

ACKNOWLEDGMENTS

The authors wish to acknowledge William Grosshandler and Kenneth Steckler from the Building and Fire Research Laboratory, Steven Brown from the Physics Laboratory at NIST, and Bror Persson, SP Swedish National and Testing Institute, Sweden, for useful discussions.

REFERENCES

1. Murthy, A. V., Tsai, B. K., and Saunders, R. D., Radiative calibration of heat flux sensors at NIST - an overview, HTD-Vol. 353, *Proceedings of the ASME Heat Transfer Division*, Vol. 3, pp. 159-164, 1997.
2. Murthy, A. V., Tsai, B. K., Transfer calibration of heat flux sensors at NIST, HTD-Vol. 345, *ASME proceedings of the National Heat Transfer Conference*, Vol. 7, Edited by Kaminski, D., Smith, A. M. and Smith, T. F., pp. 81-88, 1997.
3. Gentile, T. T., Houston, J. M., Hardis, J. E., Cromer, C. L., and Parr, A. C., The NIST high accuracy cryogenic radiometer, *Applied Optics*, Vol. 35, pp. 1056-1068, 1996.
4. Olsson, Soren, Calibration of thermal radiometers - The development of a new method. SP Report 1989:04, National Testing and Research Institute, SP, Sweden, 1989.
5. Olsson, Soren, Calibration of radiant heat flux meters - The development of a water cooled aperture for use with blackbody cavities, SP Report 1991:58, Swedish National Testing and Research Institute, Sweden, 1991.
6. Gouffé, Andre, Corrections d'ouverture des corps-noir artificiels compte tenu des diffusions multiples internes, *Revue d'Optique*, 24, 1, 1945.
7. Siegel, Robert and Howell, John R., *Thermal radiation heat transfer*, Hemisphere Publishing Corporation, Washington, 1992.
8. Kidd, C. T., and Nelson, C. G., How the Schmidt-Boelter Gage really works, *Proceedings of the 41st International Instrumentation Symposium*, pp. 347-368, 1995.
9. Murthy, A. V., Tsai, B. K., and Saunders, R. D., High heat flux sensor calibration using blackbody radiation, *Metrologia (to appear)*, 1998.

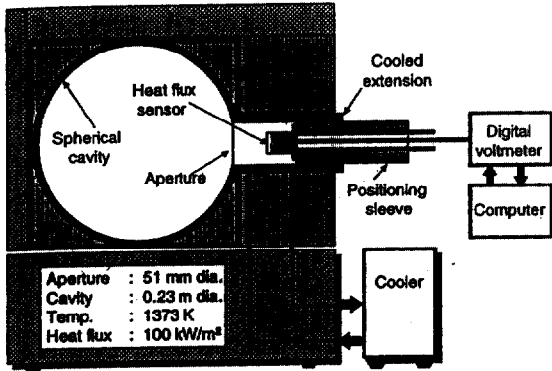


Figure 1. Schematic layout of spherical blackbody with cooled aperture.

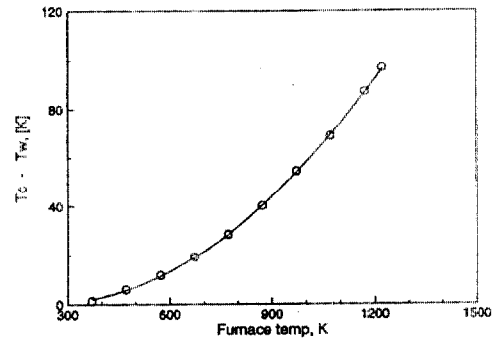


Figure 4. Cooler temperature as a function of furnace temperature.

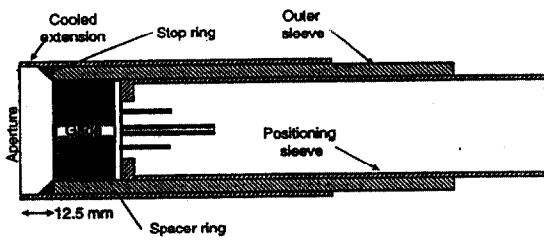


Figure 2. Water cooled extension and gage housing for the spherical blackbody.

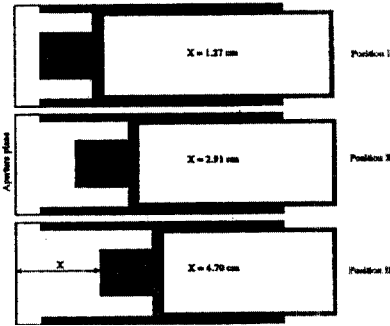


Figure 5. Gage locations in the cooled enclosure of the spherical blackbody.

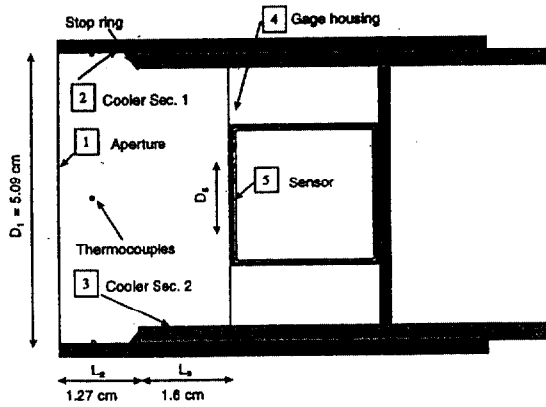


Figure 3. Schematic representation of the enclosure geometry.

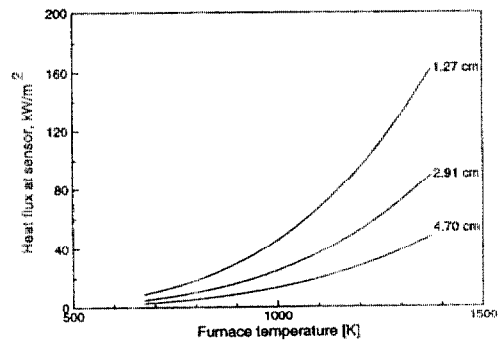


Figure 6. Enclosure radiation balance results for heat flux at sensor location.

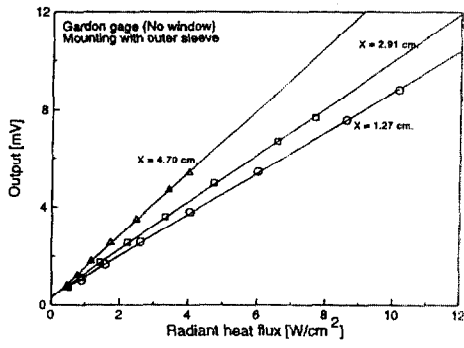


Figure 7. Results of Gardon gage calibration with outer sleeve (no venting).

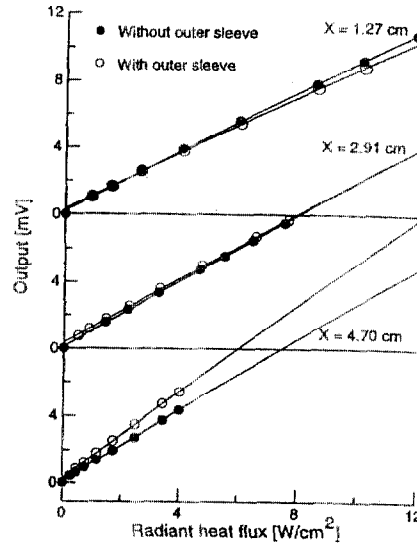


Figure 9. Effect of venting on Gardon gage output at various locations.

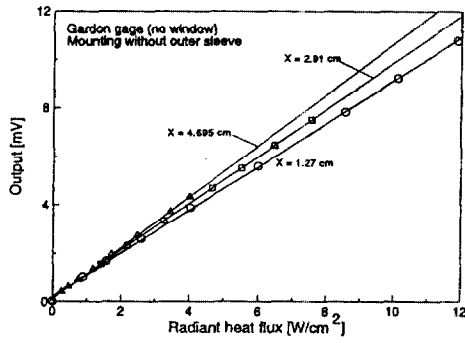


Figure 8. Results of Gardon gage calibration without outer sleeve (with venting).

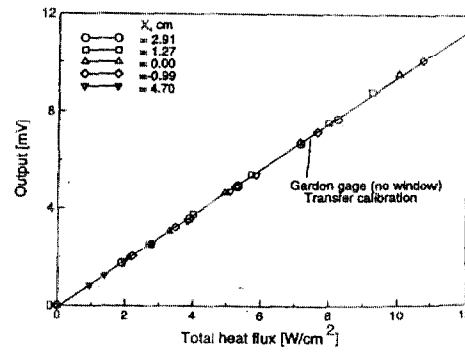


Figure 10. Transfer calibration of Gardon gage with reference to a calibrated Schmidt-Boelter sensor.